Obesity and Insulin Resistance Induce Early Development of Diastolic Dysfunction in Young Female Mice Fed a Western Diet

Camila Manrique, Vincent G. DeMarco, Annayya R. Aroor, Irina Mugerfeld, Mona Garro, Javad Habibi, Melvin R. Hayden, and James R. Sowers

Diabetes and Cardiovascular Center (C.M., V.G.D., A.R.A., I.M., M.G., J.H.,. M.R.H., J.R.S.) and Departments of Internal Medicine (C.M., V.G.D., A.R.A., I.M., M.G., J.H., M.R.H., J.R.S.) Medical Pharmacology and Physiology (V.G.D., J.R.S.), University of Missouri, Columbia, Missouri 65212 and Harry S. Truman Veterans' Administration Medical Center (J.R.S.), Columbia, Missouri 65201

Cardiovascular disease (CVD), including heart failure, constitutes the main source of morbidity and mortality in men and women with diabetes. Although healthy young women are protected against CVD, postmenopausal and diabetic women lose this CVD protection. Obesity, insulin resistance, and diabetes promote heart failure in females, and diastolic dysfunction is the earliest manifestation of this heart failure. To examine the mechanisms promoting diastolic dysfunction in insulin-resistant females, this investigation evaluated the impact of 8 weeks of a high-fructose/high-fat Western diet (WD) on insulin sensitivity and cardiac structure and function in young C57BL6/J female versus male mice. Insulin sensitivity was determined by hyperinsulinemic-euglycemic clamps and two-dimensional echocardiograms were used to evaluate cardiac function. Both males and females developed systemic insulin resistance after 8 weeks of a WD. However, only the females developed diastolic dysfunction. The diastolic dysfunction promoted by the WD was accompanied by increases in collagen 1, a marker of stiffness, increased oxidative stress, reduced insulin metabolic signaling, and increased mitochondria and cardiac microvascular alterations as determined by electron microscopy. Aldosterone (a promoter of cardiac stiffness) levels were higher in females compared with males but were not affected by the WD in either gender. These data suggest a predisposition toward developing early diastolic heart failure in females exposed to a WD. These data are consistent with the notion that higher aldosterone levels, in concert with insulin resistance, may promote myocardial stiffness and diastolic dysfunction in response to overnutrition in females. (***Endocrinology*** **154: 3632–3642, 2013)**

The prevalence of obesity, diabetes, and heart failure continues to increase in the United States and worldwide due, in part, to consumption of a Western diet (WD) high in fructose and fat content (1, 2). It is estimated that 70%–75% of premature deaths in patients with diabetes can be attributed to cardiovascular disease (CVD) (3). Diabetic women exhibit higher incidence of CVD complications compared with diabetic men (3–5), despite that nondiabetic premenopausal women exhibit less incidence of CVD compared with age-matched men. Obesity, insulin resistance, and diabetes all contribute to the increase in heart failure, especially in westernized nations (1, 2, 6–8). Diastolic dysfunction is an early finding in the natural history of obesity and diabetic cardiomyopathy and is increasingly prevalent especially in women (1, 2, 6–8). Diabetic women exhibit higher incidence of CVD complications compared with diabetic men (3–5), despite the fact that nondiabetic premenopausal women exhibit less CVD compared with age-matched men (4). Obesity, in the set-

ISSN Print 0013-7227 ISSN Online 1945-7170
Printed in U.S.A.

Received March 18, 2013. Accepted July 16, 2013.
First Published Online July 24, 2013

Abbreviations: Akt, protein kinase B; CD, control diet; CD-F, CD females; CD-M, CD males; CoA, coenzyme A; Col, collagen; COX4, cytochrome c oxidase subunit IV isoform 1; CS, citrate synthase; CVD, cardiovascular disease; DM2, type 2 diabetes; DTNB, 5,5′-dithiobis(2-nitrobenzoic acid); eNOS, endothelial nitric oxide synthase; GIR, glucose infusion rate; β-HAD, β-hydroxyacyl-CoA dehydrogenase activity; IMF, intermyofibrillar; LV, left ventricle; MPI, myocardial performance index; MR, mineralocorticoid receptor; NADH, reduced nicotinamide adenine dinucleotide; 3-NT, 3-nitrotyrosine; OXPHOS, oxidative phosphorylation; PLB, phospholamban; SERCA2, sarcoendoplasmic reticulum calcium transport ATPase; TEM, transmission electron microscopy; Vp, propagation velocity; WD, Western diet.

ting of type 2 diabetes (DM2), has a more deleterious impact on diastolic dysfunction in women than in men (8–11), and nondiabetic obese women also display increased risk for cardiac diastolic dysfunction (12–15). Population-based studies have documented higher ventricular and peripheral arterial stiffness in women, independent of body weight, as a potential factor contributing to increased incidence of diastolic dysfunction in obese females (12, 13). Further, left ventricular (LV) mass correlates positively with insulin resistance and glucose intolerance, especially in women (15).

Although the reason for the loss of CVD protection in obese and insulin-resistant women has not been established, it is likely that this is explained, in part, by the loss of the beneficial actions of estrogen that occurs with diet-induced insulin resistance and obesity (4). Indeed, reduced cardiac insulin sensitivity has been associated with structural and functional alterations that characterize diastolic dysfunction (1, 2). These abnormalities include increased interstitial fibrosis and cardiac stiffening (1, 2). In the Framingham study, aldosterone levels were found to be higher in women and to be positively associated with markers of concentric remodeling like LV wall thickness in females but not in males (16). In this regard, aldosterone also promotes fibrosis and cardiac stiffness (2). Nonetheless, the precise mechanisms by which insulin resistance/obesity contributes to the loss of estrogen protection against cardiac stiffness and diastolic dysfunction remains poorly understood.

In the present investigation, we fed a WD high in fat and fructose corn syrup to 4-week-old female and male C57BL6/J mice for 8 weeks in order to determine whether female mice are at greater risk for development of heart failure compared with males. Systemic insulin resistance was evaluated by hyperinsulinemic-euglycemic clamps. Functional outcomes investigated include echocardiographic parameters of cardiac function. The sex-related differential effects of the WD on cardiac function was then examined in relation to sex differences in systemic insulin resistance, aldosterone levels, and myocardial insulin metabolic signaling, oxidative stress, intracellular calcium (Ca^{2+}) handling proteins, and ventricular fibrosis.

Materials and Methods

Animals

All animal procedures were performed in accordance with the Animal Use and Care Committee at the University of Missouri-Columbia and National Institutes of Health guidelines. C57BL6/J males and females were obtained from The Jackson Laboratory. Groups of 4-week-old male and female mice were fed a WD consisting of high fat (46%) and high carbohydrate as sucrose (17.5%) and high-fructose corn syrup (17.5%) for 8 weeks (Test Diet 58Y1). Parallel groups of age-matched male and female controls were fed regular mouse chow for the same period of time (Test Diet 58Y2). Both cohorts were provided water ad libitum while housed in pairs under a 12-hour/day illumination regimen.

Body composition

Body composition was assessed by nuclear magnetic resonance spectroscopy in both groups after the feeding intervention at Vanderbilt University School of Medicine Mouse Metabolic Phenotyping Center.

Assessment of whole-body insulin sensitivity by hyperinsulinemic-euglycemic clamps

After the 8-week feeding trial, male and female mice underwent hyperinsulinemic-euglycemic clamps (2.5 $mU/kg^{-1}{\cdot}min^{-1}$ insulin) at the Vanderbilt University School of Medicine Mouse Metabolic Phenotyping Center as previously described (17). Five days before the study, carotid artery and jugular vein catheters were placed for blood sampling and infusion. Clamp studies were only performed on mice that weighed within 10% of presurgical body weight.

Aldosterone and leptin levels

Aldosterone levels were analyzed on plasma collected at the time of killing. Samples were analyzed in duplicate using RIA at Vanderbilt University School of Medicine Mouse Metabolic Phenotyping Center as previously described (18). Leptin levels were obtained from pooled plasma samples obtained during the clamp procedure and were quantified by RIA (Millipore).

Echocardiography protocol

Two-dimensional echocardiograms were performed in the apical 4-chamber view. The myocardial performance index (MPI), also known as the MPI index, was calculated as the sum of isovolumic contraction and relaxation times divided by ejection time. The time from cessation of the mitral valve A wave to the onset of the mitral valve E wave of the next cardiac cycle (a) is equal to the total isovolumic time plus the ejection time (b). The MPI was calculated therefore by the formula (a − b)/b. This was obtained from the apical 4-chamber view, with pulsed-wave Doppler by placing a small sample volume at the level of the LV outflow tract. Early transmitral peak diastolic flow velocity (E wave) was obtained from the same pulsed-wave Doppler spectrograms. All Doppler spectra were recorded for 5–8 cardiac cycles at a sweep speed of 200 mm/sec. Finally, to evaluate the propagation velocity (Vp) of LV inflow, a correlate of the rate of chamber relaxation, we performed color M-mode recordings of mitral inflow during early diastole at the mitral leaflets in an apical window. Parameters were assessed using an average of 3 beats from 3 different spectra, and calculations were made in accordance with the American Society of Echocardiography guidelines as well as specific guidelines for rodent echocardiography. All data were acquired and analyzed by a single blinded observer using Echo PAC (GE Vingmed) offline processing.

Heart mitochondrial function

Homogenate preparation

Briefly, whole-heart samples were homogenized with a glass tissue grinder in homogenization buffer containing 20mM HEPES (pH 7.5), 2.5mM sodium pyrophosphate, 1mM sodium orthovanadate, 1mM EDTA, 10mM glycerophosphate, 25mM sodium fluoride, 100nM okadaic acid, 250mM sucrose, and protease inhibitor cocktail (P8340; Sigma) and then passed through a 25-gauge needle. Aliquots were saved for enzymatic assays. For Western blottings, homogenates were further processed by the addition of Triton X-100 and sodium dodecyl sulfate (final concentration, 1%) and sodium chloride (final concentration, 150μM). Homogenates were incubated at 4°C with agitation for 1 hour and then centrifuged at 12 000*g* for 10 minutes. Supernatant was saved as the cytosolic fraction, and protein concentrations were determined using a Pierce BCA protein assay kit (23225; Thermo Scientific).

β-Hydroxyacyl-coenzyme A (CoA) dehydrogenase activity (β-HAD)

β-HAD enzyme is involved in mitochondrial fatty acid β-oxidation. β-HAD activity was measured as previously described with modifications (19). Heart whole-cell lysate was incubated in assay buffer containing 0.1M triethanolamine-HCl, 6.4mM EDTA, and 0.45mM reduced nicotinamide adenine dinucleotide (NADH) (pH 7.0) at 37°C. After an initial 2-minute absorbance reading at 340 nm, the reaction was initiated by adding 0.15mM acetoacetyl-CoA, and the rates of disappearance of NAD (NADH) were measured by the changes in absorbance at 340 nm every 12 seconds for 6.2 minutes. Maximum slope was calculated, adjusted for protein concentration, and used as the indication of β-HAD activity. The amount of NADH converted per minute was determined with the molar extinction coefficient for NADH. Enzyme activity was expressed as nanomoles per milligram of protein per minute.

Citrate synthase (CS) activity

CS activity was used to assess mitochondrial aerobic capacity (20) as previously described (21) with modifications. Whole-cell lysate was obtained as described above. Whole-cell lysate was incubated with buffer containing 82.4mM Tris (pH 8.3), 0.59mM oxaloacetate, and 0.12mM 5,5′-dithio-bis(2-nitrobenzoic acid) (DTNB) at 37°C for 7 minutes. The reaction was initiated with 0.43mM acetyl-CoA, and spectrophotometric detection of reduced DTNB at 405 nm was measured every 20 seconds 22 times. The maximum slope was calculated, adjusted for protein concentration. The amount of DTNB converted per minute was determined with the molar extinction coefficient for DTNB.

Ultrastructure analysis with transmission electron microscopy (TEM)

LV tissue was thinly sliced and placed in primary TEM fixative as previously described (22). After secondary fixation, specimens were placed on a rocker overnight, embedded, and polymerized at 60°C for 24 hours. Thin sections (85 nm) were then stained with 5% uranyl acetate and Sato's Triple lead stain. A JOEL 1400-EX TEM was used to view all samples. Details of LV tissue preparation, sectioning, staining, and viewing are as previously described (22).

Heart immunoblot analysis

Cytosolic fractions (30 μg per lane) were separated by SDS-PAGE and transferred to nitrocellulose (Bio-Rad Laboratories). The blots were blocked with 5% BSA in Tris-buffered saline with 1% Tween 20 at room temperature, then incubated 1 hour at room temperature with primary antibodies (1:1000 dilution) in 5% BSA, rinsed with Tris-buffered saline with 1% Tween 20, and incubated with horseradish peroxidase-conjugated secondary antibodies (1:30 000 dilution) in 5% BSA for 1 hour at room temperature. The binding of the antibodies was detected by chemiluminescence (SuperSignal West Femto, Thermo Fischer Scientific), and images were recorded using a Bio-Rad ChemiDoc XRS image analysis system. Western blot analyses were performed on phosphorylated protein kinase B (Akt)^{T308} and total Akt (Cell Signaling Technology Inc) sarcoendoplasmic reticulum calcium transport ATPase (SERCA2) (ab2861; Abcam), 3-nitrotyrosine (3-NT) (AB5411; EMD Millipore, Billerica, Massachusetts), collagen (Col) 1A1 (sc-8784; Santa Cruz Biotechnology, Inc), and Col 3A (sc-8781; Santa Cruz Biotechnology, Inc). Quantitation of protein band density, normalized to the density of pan-actin (4968; Cell Signaling Technology, Inc) or amido black for each sample, was performed using Image Lab software (Bio-Rad Laboratories). Data are reported as the normalized protein band density in arbitrary units.

Statistical analysis

Results are reported as the mean ± SE. Differences in outcomes were determined using two-way ANOVA or paired *t* tests and were considered significant when $P < .05$. All statistical analyses were performed using Sigma Plot (version 12) software (Systat Software).

Results

WD promotes obesity and insulin resistance in female mice

The average body weight of female mice fed a control diet (CD) was less than males (20.0 ± 0.3 vs 24.2 ± 0.4 g, respectively; $P < .05$), and the WD induced a 22% increase in body weight in both female and male mice (24.5 ± 0.8 vs 29.7 ± 1.3 g, respectively; $P < .05$). Body composition was assessed in the different cohorts by nuclear magnetic resonance spectroscopy. CD males (CD-M) had a trend toward lesser body fat than CD females (CD-F) (CD-M, 13.62 ± 1.07 vs CD-F, 17.35 ± 1.76%; $P = .08$). WD only increased body fat percentage significantly in WD-M but not in WD-F (CD-M, 13.62 ± 1.07 vs WD-M, 20.16 ± 2.11%; $P < .01$; CD-F, 17.35 ± 1.76 vs WD-F, 18.23 ± 1.01%; $P = .67$). Leptin was significantly elevated in female mice, and there was a trend toward increased leptin levels in both sexes upon WD feeding (Table 1). Heart weight was smaller in female mice on CD compared with males (86 ± 0.9 vs 99 ± 1 mg, respectively; $P < .05$), and WD induced an increase in heart weight in males (113 ± 0.6 mg; $P < .05$) but not female mice (99 ± 2.5 mg; $P >$

TABLE 1. Effect of WD on Plasma Leptin Levels

Parameter	Main effect	*P* value	CD-F (8)	WD-F (9)	CD-M (6)	WD-M (6)
Plasma leptin (ng/mL)						
Sex		0.003	6.56[a]	8.52[b]	3.01	4.71
Diet		0.081	±0.97	±1.69	±0.59	±0.97
Interaction		0.761				

Leptin levels tended to be higher in both sexes fed a WD. However, the differences did not reach significance. Values are mean ± SE. Numbers in parentheses are sample sizes.

[a] Sex within control.

[b] Sex within WD.

.05). There was also an increase in heart weight normalized to tibia length in WD-M compared with CD-M (67 ± 2 vs 57 ± 2 mg/cm; $P < .05$) but not WD-F compared with CD-F (53 ± 1 vs 51 ± 1 mg/cm; $P > .05$). Tibia length did not vary significantly among groups. This demonstrates that a WD induced cardiac hypertrophy in males but not females. In a separate cohort of mice, systemic glucose sensitivity was assessed by hyperinsulinemic-euglycemic clamps. Steady state glucose infusion rates (GIRs) during clamps were significantly higher in CD-F compared with their CD-M counterparts, demonstrating greater whole-body insulin sensitivity in normal females ($P < .05$) (Figure 1, A and B). Both male and female mice fed a WD exhibit reduced GIR compared with male and female mice fed a CD, indicating significant insulin resistance ($P < .05$) (Figure 1, A and B). Unlike in the control groups, the GIRs were similar for both sexes fed a WD, suggesting that insulin sensitivity in females is more impaired by WD than in males.

WD induces diastolic dysfunction in female but not male mice

Female mice fed a WD for 8 weeks exhibit abnormal echocardiographic diastolic function parameters when compared with their male counterparts (Figure 2, A–D). The MPI, which assesses both systolic and diastolic function, was increased in both sexes fed a WD, but its impact was greater in females (Figure 2A and Supplemental Table 1, published on The Endocrine Society's Journals Online web site at http://endo.endojournals.org). It should be noted that an increase in this parameter is indicative of impaired cardiac function. The increase in MPI in WD-F compared with CD-F is likely due to abnormal diastolic function as indicated by both a prolonged period of isovolumic relaxation ($P < .05$) (Figure 2B) and a decrease in mitral inflow Vp ($P = .06$) (Figure 2C). The E/Vp ratio, a marker of LV filling pressure, was elevated in the WD-F compared with CD-F (Figure 2D) and further supports the diagnosis of diastolic dysfunction.

WD induces myocardial oxidative stress in female mice

Excessive myocardial oxidative stress has been linked to heart failure in different experimental models (23–25). The nitration of protein tyrosine residues can be evaluated by 3-NT immunostaining and is an indirect marker of increased peroxynitrite formation and oxidative stress. The basal level of myocardial 3-NT in female mice was lower than in male mice. WD induces increased myocardial 3-NT staining in both male and female mice. However, the relative increase in 3-NT

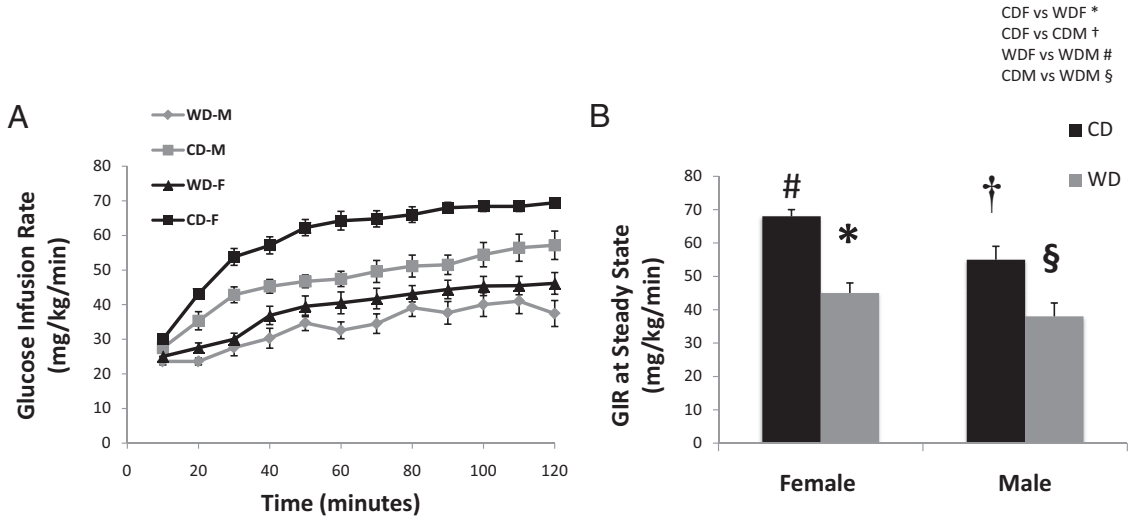

Figure 1. WD promotes insulin resistance in both sexes and especially in female mice. (A) GIR during the hyperinsulinemic-euglycemic clamp after 8 weeks of feeding. (B) GIR at steady state (80–120 min). Sample sizes are 9, 9, 7, and 8 for CD-F, WD-F, CD-M, and WD-M. Values are means ± SE. Post hoc comparisons: *,CD-F vs WD-F; †, CD-F vs CD-M; #, WD-F vs WD-M, §, CD-M vs WD-M.

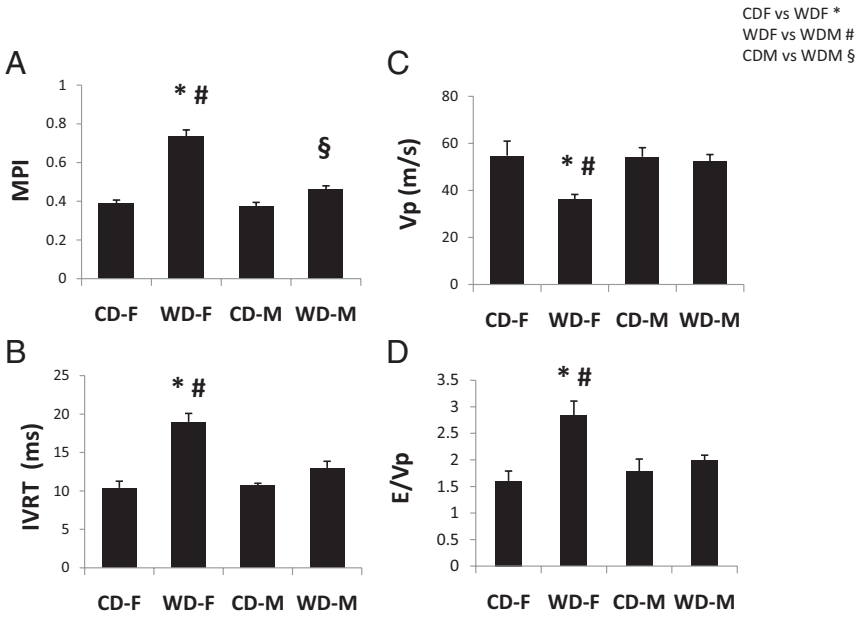

Figure 2. WD induces diastolic dysfunction in female mice. Bar graphs show (A) MPI, (B) isovolumic relaxation time (IVRT), (C) Vp, and (D) E/Vp ratio, an index of LV filling pressure. Sample sizes are 5, 5, 3, and 3 for CD-F, WD-F, CD-M, and WD-M, respectively. Values are means ± SE. Post hoc comparisons: *, CD-F vs WD-F; #, WD-F vs WD-M; §, CD-M vs WD-M.

caused by WD was greater in females than males (females: 55%, $P < .05$; males, 17%; $P = .06$) (Figure 3). Sex had a significant effect on 3-NT levels, demonstrating higher levels of oxidative stress in male mice regardless of feeding regime.

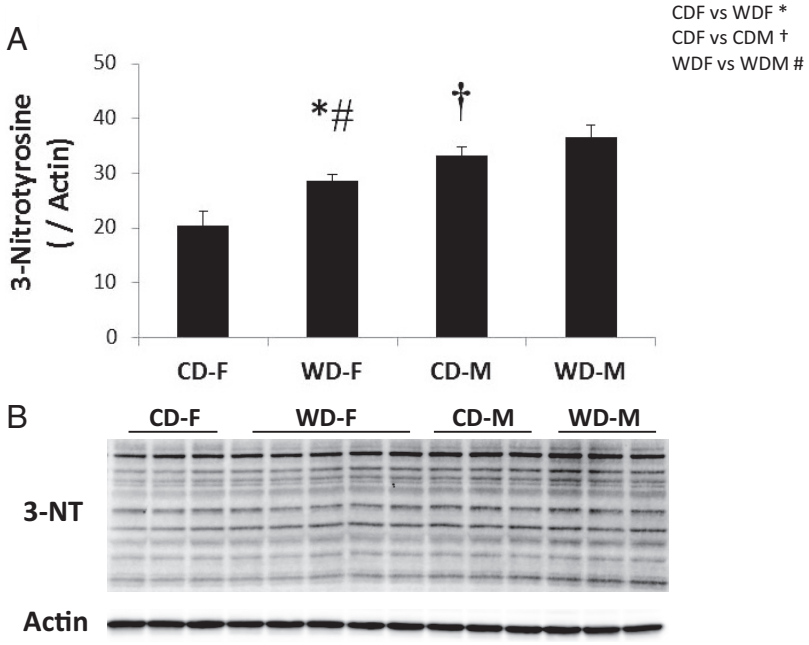

Figure 3. WD induces myocardial oxidative stress in female mice. (A) The bar graph shows the level of 3-NT immunostaining in samples of LV homogenates. CD-F, n = 5; CD-M, n = 3; WD-F, n = 5; WD-M, n = 3. Sample sizes are 5, 5, 3, and 3 for CD-F, WD-F, CD-M, and WD-M, respectively. Values are means ± SE. Post hoc comparisons: *, CD-F vs WD-F; †, CD-F vs CD-M; #, WD-F vs WD-M.

WD alters myocardial Col content and composition

Immunoblotting was used to examine the expression of Col isoforms in the different treatment groups. The expression of Col 1A1 (Col 1) (Col component that most determines stiffness) was increased in WD-F compared with CD-F ($P < .05$) (Figure 4A). Col 3A (Col 3) expression did not vary among treatment groups (Figure 4B). Importantly, there was an increase in the ratio of Col 1 to Col 3 in WD-F compared with CD-F ($P < .05$) (Figure 4C), and this alteration in myocardial composition of Col (relative increase in Col 1) reflects a more stiff and a less compliant LV (26).

WD impairs Ca^{2+} cycling protein expression in females

To explore the mechanisms contributing to impaired diastolic function in the female mice fed a WD, we examined the expression levels of SERCA2a, and phospholamban (PLB), proteins known to modulate Ca^{2+} handling and cycling (1, 2). Total PLB expression did not vary with sex or diet (Figure 5A). Trends suggested that the relative expression of SERCA2a decreased in WD-F compared with CD-F and increased in WD-M compared with CD-M, although neither trend was significant (Figure 5B). The ratio of PLB to SERCA2a was elevated in WD-F compared with CD-F ($P < .05$) and tended to decrease in WD-M compared with CD-M ($P = .07$) (Figure 5C), suggestive of impaired Ca^{2+} handling in WD-F and compensatory improvement of Ca^{2+} handling in WD-M. We also determined phosphorylation of PLB at Ser^{16} and Thr^{17} residues, and they were not significantly different among groups (data not shown).

WD effects on mitochondrial function

We determined the activities of CS, a Kreb's cycle enzyme used to

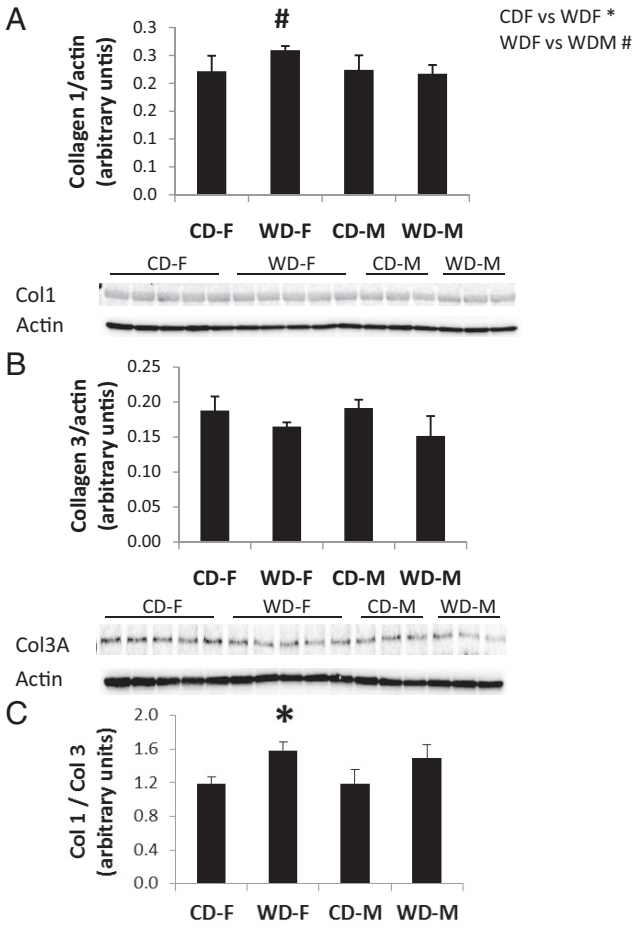

Figure 4. WD alters myocardial Col content and composition. Immunoblotting was used to examine the relative expression of (A) Col 1 and (B) Col 3 protein. Protein loading was normalized to actin, and Col and actin bands are shown below bar graphs. The ratio of Col 1 to Col 3 is shown in C. Post hoc comparisons: *, CD-F vs WD-F; #, WD-F vs WD-M.

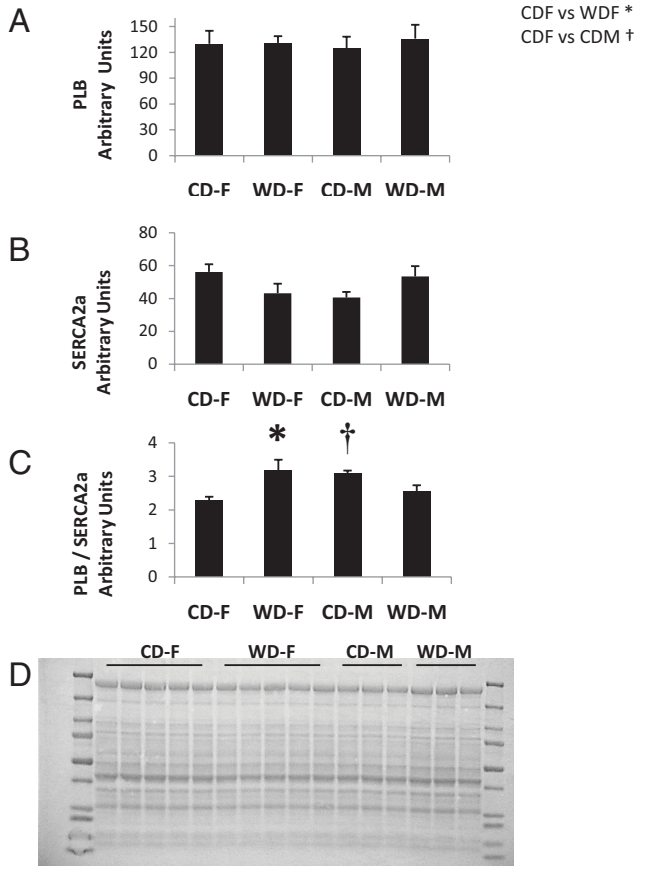

Figure 5. WD impairs Ca^{2+} cycling protein expression in female mice. Bar graphs show the protein expression levels of (A) PLB, (B) SERCA2a, and (C) the ratio of PLB to SERCA2. Protein loading was normalized to amido black staining shown in D. Sample sizes are 5, 5, 3, and 3 for CD-F, WD-F, CD-M, and WD-M, respectively. Values are means ± SE. Post hoc comparisons: *, CD-F vs WD-F; †, CD-F vs CD-M.

assess aerobic capacity of mitochondria, and β-HAD, an enzyme involved in mitochondrial fatty acid β-oxidation in LV homogenates. In CD-F, activity of CS was significantly lower than in CD-M ($P < .05$) (Figure 6A). In the WD-treated groups, CS activity was marginally lower in the female mice but not in males. Similar to CS activity, the activity of β-HAD in CD-F mice was lower than in CD-M ($P < .05$) (Figure 6B). In contrast, β-HAD activity was marginally increased in WD-F compared with CD-F, whereas the WD did not affect β-HAD activity in males. Immunoblotting was performed to determine the changes in the levels of electron transport chain components oxidative phosphorylation (OXPHOS) and cytochrome c oxidase subunit IV isoform 1 (COX4). Relative protein expression levels of mitochondrial COX4 and OXPHOS I–III and V did not differ between the different intervention groups (data not shown).

Decreased Akt activation by WD in female mice

The phosphorylation of Akt at the Thr^{308} residue was significantly higher in CD-F compared with CD-M ($P < .05$) (Figure 7A). However, total Akt protein levels did not differ between these 2 groups (Figure 7B). Although Akt phosphorylation was not significantly decreased in males fed a WD compared with males fed a CD, the levels were markedly lower in WD-fed females compared with females fed a CD ($P < .0\%$) (Figure 7A). Total Akt levels in mice fed a CD did not differ between males and females, although total Akt was lower in WD-M compared with WD-F and CD-M ($P < .05$). We examined the phosphorylation of endothelial nitric oxide synthase (eNOS) at the Ser^{1177} residue, because it is one of the downstream substrates of Akt. However, the levels of phosphorylated eNOS tended to be lower in females fed a CD compared with males ($P = .09$), as well as in females fed a WD compared with males ($P = .07$). Total eNOS levels were decreased in WD-fed females compared with CD-fed females and WD males ($P < .05$). These results suggest that both phosphorylated eNOS and total eNOS were lower in

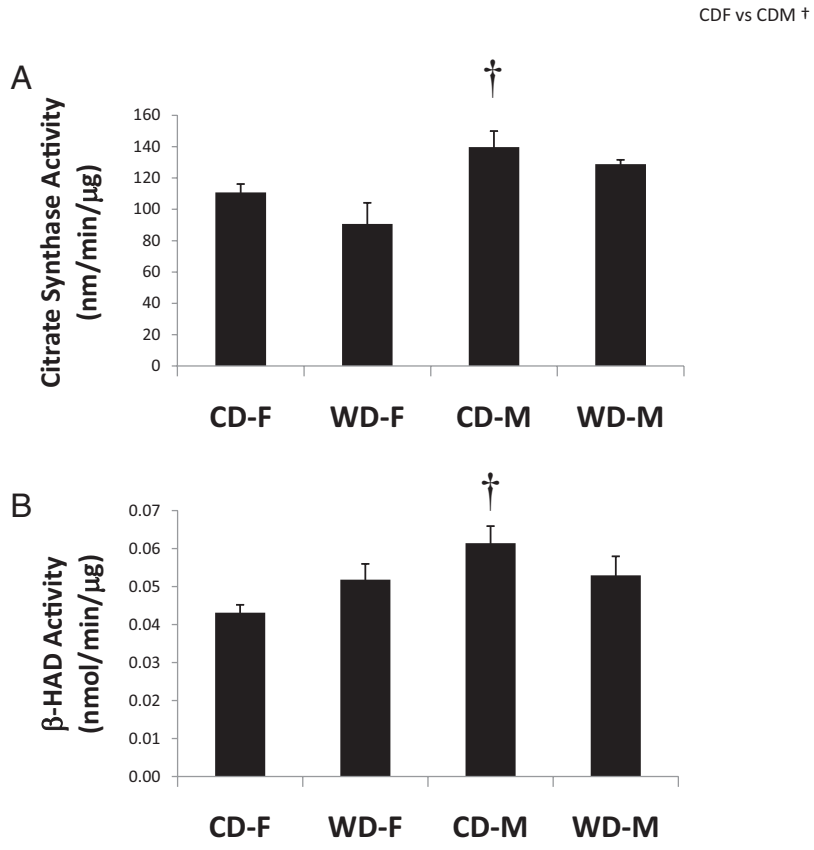

Figure 6. Effect of WD on mitochondrial enzyme activities. Bar graphs show (A) CS and (B) β-HAD activities in LV homogenates. Sample sizes are 5, 5, 3, and 3 for CD-F, WD-F, CD-M, and WD-M, respectively. Values are means ± SE. Post hoc comparisons: †, CD-F vs CD-M.

WD-fed females compared with females fed a CD. These patterns were not apparent in males.

Abnormalities in myocardial ultrastructure by WD in female mice

TEM was used to examine myocardial ultrastructure in the different cohorts as previously described in detail (22). Female and male mice fed a WD exhibited increased intermyofibrillar (IMF) mitochondria when compared with control fed counterparts (Figure 8). Female mice on WD demonstrated capillary endothelial cell cytoplasm thinning and attenuation of transcytotic endothelial vesicles as well as fenestra formation in comparison with the other groups. These ultrastructural observations may indicate immature capillaries that may be associated with increased angiogenesis. These ultrastructural remodeling changes may be associated with the decrease in myocardial eNOS levels observed in WD females.

WD effects on plasma aldosterone levels

There was a significant effect of sex demonstrating significantly higher aldosterone levels in females compared with males ($P < .05$). Feeding regime had no effect on aldosterone levels within each sex ($P > .05$). Specifically, plasma aldosterone levels in CD-F and WD-F were 648 ± 82 and 635 ± 49 pg/mL, respectively ($P > .05$) and in CD-M and WD-M mice plasma aldosterone levels were 392 ± 31 and 408 ± 45 pg/mL, respectively ($P > .05$)

Discussion

Overnutrition and obesity are the driving force behind the current epidemic of DM2 and associated heart failure due, in part, to the consumption of a WD high in fructose and fat (27, 28). Insulin resistance in obesity and DM2 contributes to heart failure manifested initially as diastolic dysfunction (29, 30). Although nonobese young women exhibit enhanced insulin sensitivity compared with young men, young women are at greater risk for development of heart failure in conditions of overnutrition/obesity (8–11). In this investigation, we determined the effects of a diet high in fat and fructose that closely resembles the widespread dietary pattern in the Western world. These studies demonstrate that feeding a WD to young female C57BL6/J mice causes diastolic dysfunction in as few as 8 weeks on the experimental diet and abrogates the enhanced whole-body insulin sensitivity seen in female compared with male mice fed a CD without significantly impacting body fat composition. Consistent with human studies, the female mice studied here demonstrated higher leptin levels (31), and WD feeding tended to increase leptin even further. Plasma leptin levels have been negatively associated with markers of diastolic function in obese patients (32). We speculate that the elevated leptin levels observed in the young WD-fed females induce an increase in sympatho-adrenergic tone that contributes to the early development of the cardiac phenotype. The WD eventually induces a similar cardiac phenotype in male mice that we have observed after 12 weeks on the diet (our unpublished data). Because we began feeding mice a WD at a very young age (4 wk of age) and females developed diastolic function after only 8 weeks of receiving the experimental diet, this model recapitulates the common clinical problem of obesity during childhood years and adolescence, as well as the increased risk for diastolic dysfunction in obese young women (11, 14).

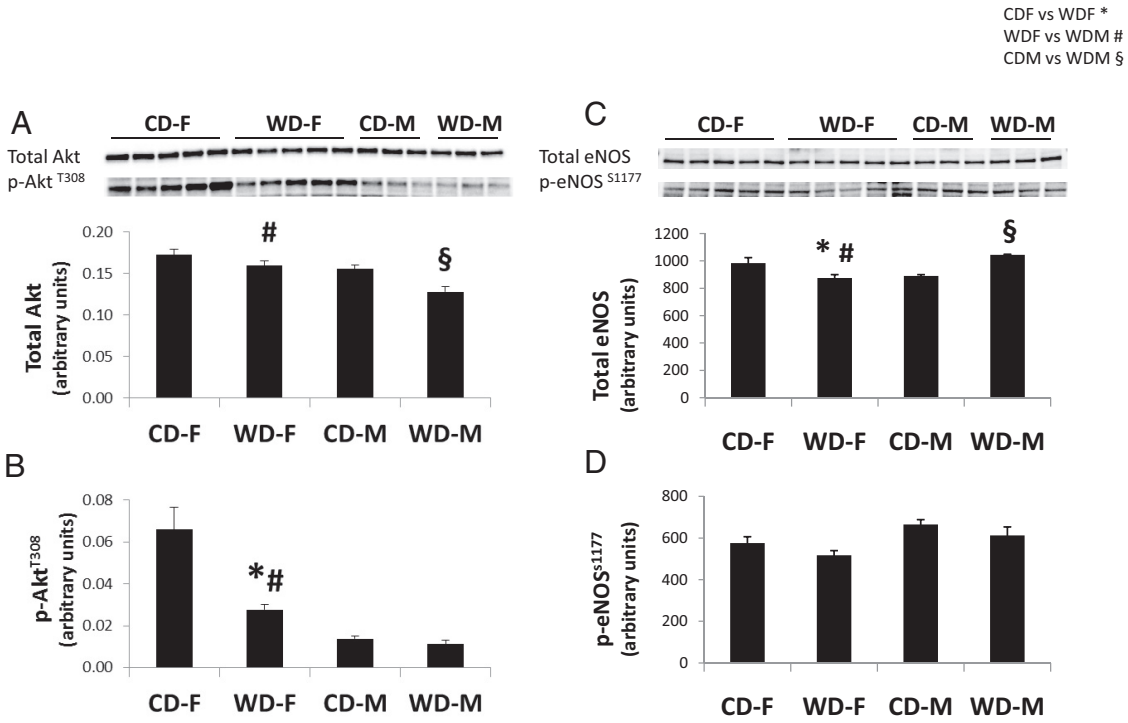

Figure 7. WD caused decreased total Akt content and activation on female LV. (A) Total Akt protein levels in myocardial homogenates from the LV decreased after 8 weeks of WD feeding in females and males. (B) Thr^{308}-phosphorylated Akt [$p\text{-}Akt^{(T308)}$] was decreased in WD-F. WD caused decreased activation of eNOS in male LV. eNOS activation was evaluated by immunoblotting of total eNOS and Ser^{1177}-phosphorylated eNOS [$p\text{-}eNOS\ (^{S1177})$]. WD feeding only significantly decreased eNOS activation in WD-M. CD-F, n = 5; CD-M, n = 3; WD-F, n = 5; WD-M, n = 3. Values are means ± SE. *, CD-F vs WD-F; #, WD-F vs WD-M; §, CD-M vs WD-M.

To clarify possible pathological mechanisms responsible for the abnormal functional findings, we explored different pathways known to be involved in diastolic dysfunction, such as LV fibrosis and hypertrophy, oxidative stress, abnormal Ca^{2+} handling, and impaired insulin (ie, Akt) and eNOS signaling. In models of metabolic/diabetic heart disease, oxidative stress has been documented to play an important role in the appearance of cardiac dysfunction (24, 25). In the absence of obesity, premenopausal women are protected against CVD risk due to high levels of estrogen. However, this protection is lost due to enhanced oxidative stress in the setting of obesity. We have previously reported a role of oxidative stress in diastolic dysfunction in different models of obesity and cardiac dysfunction, including the *db/db* mouse model (21). In this study, we show that female mice have lower myocardial oxidative stress than males in control conditions. However, consumption of a WD induced a relatively greater increase in myocardial oxidative stress in female compared with male hearts (40% vs 10% above their respective controls).

Abnormal myocardial Ca^{2+} handling has been identified as an early finding in diastolic dysfunction (6, 33). In the present study, there were no significant differences in the total content of SERCA2a, its inhibitory protein PLB, or phosphorylation of phosphorylated PLB^{ser16}. However, the ratio of PLB to SERCA2a was elevated in females on WD and tended to be reduced in males on WD. Some studies have reported nonsignificant changes in expression of either SERCA2a or PLB protein in the heart, yet changes in the ratio of these 2 proteins suggest abnormal Ca^{2+} handling (29, 30). These data suggest that the improved Ca^{2+} handling observed in males fed a WD is evidence of a compensatory response that may protect males from premature development of diastolic dysfunction. On the other hand, females are unable to compensate as males.

The composition of Col isoforms within the myocardial interstitial matrix is one of the determinants of diastolic stiffness of the LV (34, 35). Differences in the ratio of the 2 predominant myocardial Col isoforms, Col 1 and Col 3, are consequential, because a change in the ratio of these isoforms alters the passive mechanical properties of the LV wall. Col 3 is the more compliant isoform, whereas Col 1 is stronger and stiffer. In this regard, an increase in the Col 1 to Col 3 ratio denotes increased LV wall stiffness, such as would occur in a heart with diastolic dysfunction with preserved ejection fraction. On the other hand, a decrease in the ratio would be more consistent with more advanced heart failure with systolic dysfunction, such as occurs in conditions with dilated cardiomyopathy. In the present investigation, we observed an increase in the Col 1 to Col 3 ratio in the heart of female mice fed a WD, suggestive of an increase in myocardial stiffness. There was no evidence of WD-induced LV hy-

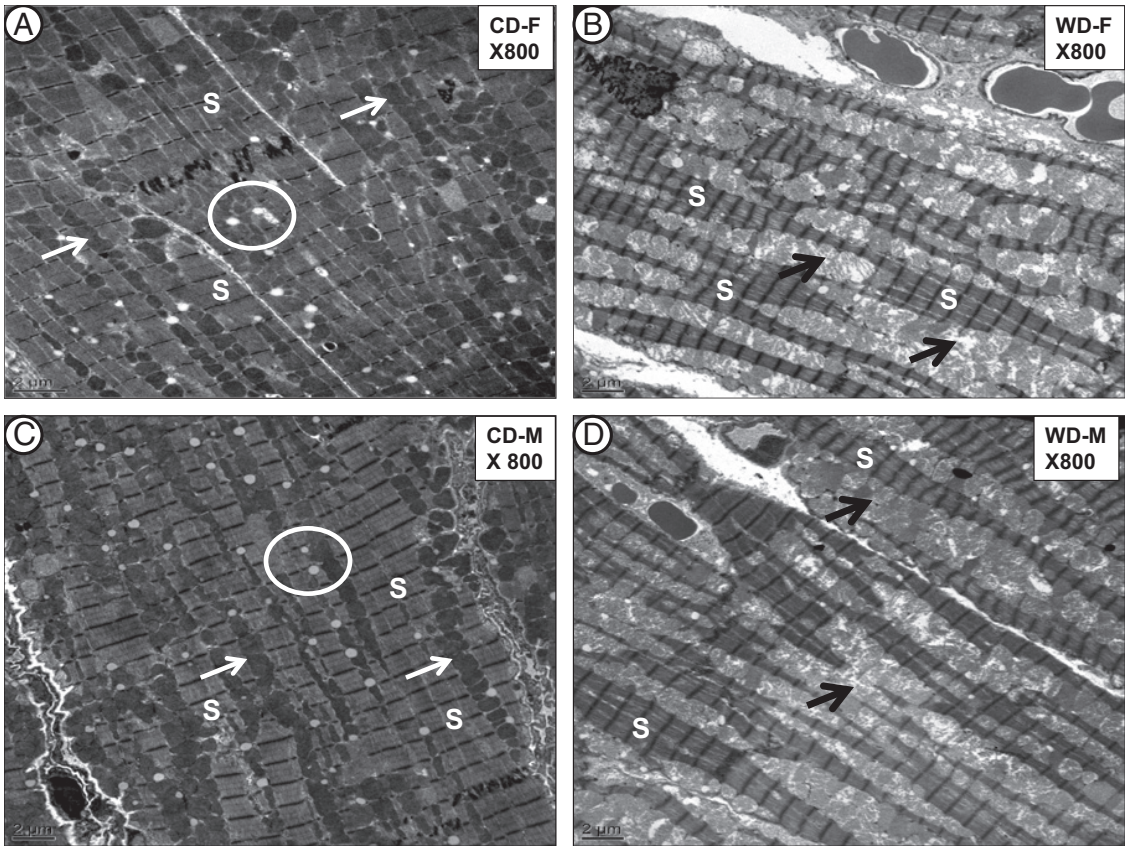

Figure 8. Effect of WD on IMF mitochondria density. WD-treated rodents exhibit a similar increase in abnormal IMF mitochondria (arrows) with loss of mitochondrial density and abnormal cristae as compared with controls (A and C). Also note that there was a decrease in electron lucent IMF lipid droplets (encircled) in regions of mitochondrial remodeling in Western models (B and D) as compared with controls (A and C). Additionally, note the disorganization and decreased volume of the sarcomeres (S). Magnification, ×800; scale bar, 2 μm.

pertrophy in female mice, although male mice fed a WD did exhibit LV hypertrophy. In this regard, the development of diastolic dysfunction has been shown to occur independent of cardiac hypertrophy (21, 36, 37).

Mitochondrial dysfunction has been associated with diastolic dysfunction in obesity models (38, 39). In the current investigation, CS activity was significantly higher in control males compared with females. The higher CS activity in males might reflect a higher metabolic capacity and potentially lesser predisposition for lipid toxicity (38). Moreover, the marginal increase in β-HAD activity and the decreasing CS activity observed in WD-fed females may suggest a relative increase in fatty acid oxidation contributing to increased oxidative stress, reduced myocardial metabolic efficiency, and diastolic dysfunction. Diastolic dysfunction has also been associated with increases, decreases, or normal mitochondrial content in models of insulin-resistant cardiomyopathy (40, 41). In this study, we examined mitochondrial function and ultrastructure. There was no significant increase in mitochondrial content as evaluated by immunoblots of OXPHOS subunits and COX4. Nonetheless, TEM examination of myocardial ultrastructure in the different treatment groups revealed an increase in the numbers of IMF mitochondria in both females and males fed a WD that were not observed in mice on CD. We have reported similar ultrastructural changes in young insulin-resistant Zucker obese rats with diastolic dysfunction (37) and in prediabetic obese *db/db* mice during the transition to diastolic dysfunction (21). In this respect, the susceptibility to oxidative stress and increased mitochondrial protein nitration has been described preferentially to IMF mitochondria (42), and this is consistent with the observed increase in the 3-NT burden in female mice fed a WD compared with males. We also observed demonstrated capillary endothelial cell cytoplasm thinning and attenuation of transcytotic endothelial vesicles as well as fenestra formation in female mice on WD in comparison with the other groups. These ultrastructural observations may indicate immature capillaries that may be associated with altered angiogenesis. These ultrastructural remodeling changes may be associated with the decrease in myocardial eNOS levels observed in WD females

Akt activation is a critical signaling node that conveys multiple different intracellular signaling pathways. Of importance, Akt activation results from normal insulin and IGF-I signaling. In models of obesity and insulin resistance, abnormalities in the insulin signaling cascade in the

heart, including decreased Akt activation, have been documented (43, 44). Furthermore, estrogen-mediated myocardial activation of Akt has been proposed to partially explain the observed sex-related differences in cardiac disease (45). In the present study, we found increased Akt phosphorylation (activation) in control female mice that markedly decreased after 8 weeks of WD. In this study, we also examined phosphorylation of eNOS as a downstream target of insulin-Akt signaling. However, we observed a marginal decrease in phosphorylated eNOS and total eNOS in WD-fed female mice. Therefore, decreased eNOS phosphorylation may account, in part, for the impairment of diastolic function in female mice fed a WD (46). Taken together, Akt signaling may be one of the signal transduction pathways contributing to impaired diastolic function and increased cardiovascular risk in obese female mice.

In a population-based study, women have higher serum levels of aldosterone that correlate with a pattern of LV concentric remodeling (16). In this study, we found that young female C57BL6 mice exhibit higher serum levels of aldosterone compared with males. Aldosterone and mineralocorticoid receptor (MR) activation has been considered as a pathogenic factor in diabetic heart disease (47). Moreover, clinical studies using MR blockade have documented a beneficial impact of MR blockade in diastolic function of women with heart failure (48). In addition, studies have shown that MR blockade in obese patients improves LV diastolic function and fibrosis markers (49, 50). We observed that WD had no effect on aldosterone levels in males or females. MR activation promotes oxidative stress and fibrosis in the myocardium (51). We observed that females fed a WD have increased myocardial oxidative stress and fibrosis compared with female mice fed a CD. This suggests that there may be increased sensitivity for aldosterone effects on oxidative stress and fibrosis under conditions of overnutrition. Therefore, the interaction of higher aldosterone levels and overnutrition may act synergistically to promote the progression of diastolic dysfunction.

In summary, the present investigation demonstrates that 8 weeks of a WD high in fat and fructose abrogates the enhanced whole-body insulin sensitivity seen in female mice fed a CD compared with males and induces early progression to diastolic dysfunction in female, but not male, C57BL6/J mice. Diastolic dysfunction in female mice was accompanied by increased myocardial oxidative stress, Col stiffness, altered Ca^{2+} handling, and a marked decrease in Akt/eNOS activation. In addition, the circulating levels of aldosterone in female mice are increased, and this raises the possibility that the systemic and myocardial metabolic effects of aldosterone are potentiated resulting in loss of systemic and myocardial insulin sensitivity and the development diastolic dysfunction.

Acknowledgments

We thank Brenda Hunter for editorial assistance and Nathan Rehmer for technical and administrative support. We also thank the Electron Microscope Core Center at the University of Missouri-Columbia for help with preparation of tissue samples and the Vanderbilt University School of Medicine Mouse Metabolic Phenotyping Center (Nashville, Tennessee) where the clamps were performed.

Address all correspondence and requests for reprints to: James R. Sowers, MD, Professor of Medicine and Medical Pharmacology and Physiology, University of Missouri, D109 Diabetes Center Health Sciences Center, One Hospital Drive, Columbia, Missouri 65212. E-mail: sowersj@health.missouri.edu.

This work was supported by the National Institutes of Health Grants R01-HL73101 and R01-HL1079100, the Veterans Affairs Merit System 0018 (to J.R.S.), and the Diabetes Cosmopolitan Foundation (C.M.).

Disclosure Summary: The authors have nothing to disclose.

References

1. **Pulakat L, Demarco VG, Whaley-Connell A, Sowers JR.** The impact of overnutrition on insulin metabolic signaling in the heart and the kidney. *Cardiorenal Med*. 2011;1:102–112.
2. **Mandavia CH, Aroor AR, Demarco VG, Sowers JR.** Molecular and metabolic mechanisms of cardiac dysfunction in diabetes. *Life Sci*. 2013;92:601–608.
3. **Huxley R, Barzi F, Woodward M.** Excess risk of fatal coronary heart disease associated with diabetes in men and women: meta-analysis of 37 prospective cohort studies. *BMJ*. 2006;332:73–78.
4. **Barrett-Connor E, Giardina EG, Gitt AK, Gudat U, Steinberg HO, Tschoepe D.** Women and heart disease: the role of diabetes and hyperglycemia. *Arch Intern Med*. 2004;164:934–942.
5. **Howard BV, Cowan LD, Go O, et al.** 1998 Adverse effects of diabetes on multiple cardiovascular disease risk factors in women. The Strong Heart Study. *Diabetes Care*. 21:1258–1265.
6. **Schilling JD, Mann DL.** Diabetic cardiomyopathy: bench to bedside. *Heart Fail Clin*. 2012;8:619–631.
7. **Schillaci G, Pirro M, Pucci G, et al.** Different impact of the metabolic syndrome on left ventricular structure and function in hypertensive men and women. *Hypertension*. 2006;47:881–886.
8. **Peterson LR, Waggoner AD, Schechtman KB, et al.** Alterations in left ventricular structure and function in young healthy obese women: assessment by echocardiography and tissue doppler imaging. *J Am Coll Cardiol*. 2004;43:1399–1404.
9. **Peterson LR, Soto PF, Herrero P, et al.** Impact of gender on the myocardial metabolic response to obesity. *JACC Cardiovasc Imaging*. 2008;1:424–433.
10. **Peterson LR, Saeed IM, McGill JB, et al.** Sex and type 2 diabetes: obesity-independent effects on left ventricular substrate metabolism and relaxation in humans. *Obesity*. 2012;20:802–810.
11. **Peterson LR, Herrero P, Schechtman KB, et al.** Effect of obesity and insulin resistance on myocardial substrate metabolism and efficiency in young women. *Circulation*. 2004;109:2191–2196.
12. **Redfield MM, Jacobsen SJ, Borlaug BA, Rodeheffer RJ, Kass DA.** Age- and gender-related ventricular-vascular stiffening: a community-based study. *Circulation*. 2005;112:2254–2262.
13. **Russo C, Jin Z, Palmieri V, et al.** Arterial stiffness and wave reflection: sex differences and relationship with left ventricular diastolic function. *Hypertension*. 2012;60:362–368.

14. **De Simone G, Devereux RB, Chinali M, et al.** Sex differences in obesity-related changes in left ventricular morphology: the Strong Heart Study. *J Hypertens*. 2011;29:1431–1438.
15. **Rutter MK, Parise H, Benjamin EJ, et al.** Impact of glucose intolerance and insulin resistance on cardiac structure and function: sex-related differences in the Framingham Heart Study. *Circulation*. 2003;107:448–454.
16. **Vasan RS, Evans JC, Benjamin EJ, et al.** Relations of serum aldosterone to cardiac structure: gender-related differences in the Framingham Heart Study. *Hypertension*. 2004;43:957–962.
17. **Ayala JE, Bracy DP, McGuinness OP, Wasserman DH.** Considerations in the design of hyperinsulinemic-euglycemic clamps in the conscious mouse. *Diabetes*. 2006;55:390–397.
18. **Luther JM, Wang Z, Ma J, Makhanova N, Kim HS, Brown NJ.** Endogenous aldosterone contributes to acute angiotensin II-stimulated plasminogen activator inhibitor-1 and preproendothelin-1 expression in heart but not aorta. *Endocrinology*. 2009;150:2229–2236.
19. **Bass A, Brdiczka D, Eyer P, Hofer S, Pette D.** Metabolic differentiation of distinct muscle types at the level of enzymatic organization. *Eur J Biochem*. 1969;10:198–206.
20. **Srere PA.** Citrate synthase. *Methods Enzymol*. 1969;13:3–5.
21. **Demarco VG, Ford DA, Henriksen EJ, et al.** Obesity-related alterations in cardiac lipid profile and nondipping blood pressure pattern during transition to diastolic dysfunction in male db/db mice. *Endocrinology*. 2013;154:159–171.
22. **Whaley-Connell A, Govindarajan G, Habibi J, et al.** Angiotensin II-mediated oxidative stress promotes myocardial tissue remodeling in the transgenic TG (mRen2) 27 Ren2 rat. *Am J Physiol Endocrinol Metab*. 2007;293:E355–E363.
23. **Tsutsui H, Kinugawa S, Matsushima S.** Oxidative stress and heart failure. *Am J Physiol Heart Circ Physiol*. 2011;301:H2181–H2190.
24. **Serpillon S, Floyd BC, Gupte RS, et al.** Superoxide production by NAD(P)H oxidase and mitochondria is increased in genetically obese and hyperglycemic rat heart and aorta before the development of cardiac dysfunction. The role of glucose-6-phosphate dehydrogenase-derived NADPH. *Am J Physiol Heart Circ Physiol*. 2009; 297:H153–H162.
25. **Shen X, Zheng S, Metreveli NS, Epstein PN.** Protection of cardiac mitochondria by overexpression of MnSOD reduces diabetic cardiomyopathy. *Diabetes*. 2006;55:798–805.
26. **Segura AM, Frazier OH, Buja LM.** Fibrosis and heart failure [published online November 4, 2012]. *Heart Fail Rev*. doi:10.1007/s10741-012-9365-4.
27. **Narayan KM, Boyle JP, Thompson TJ, Sorensen SW, Williamson DF.** Lifetime risk for diabetes mellitus in the United States. *JAMA*. 2003;290:1884–1890.
28. **Centers for Disease Control and Prevention (CDC).** Obesity prevalence among low-income, preschool-aged children–New York City and Los Angeles County, 2003–2011. *MMWR Morb Mortal Wkly Rep*. 2013;62(2):17–22.
29. **Ouwens DM, Boer C, Fodor M, et al.** Cardiac dysfunction induced by high-fat diet is associated with altered myocardial insulin signalling in rats. *Diabetologia*. 2005;48:1229–1237.
30. **Wold LE, Dutta K, Mason MM, et al.** Impaired SERCA function contributes to cardiomyocyte dysfunction in insulin resistant rats. *J Mol Cell Cardiol*. 2005;39:297–307.
31. **Couillard C, Mauriège P, Prud'homme D, et al.** Plasma leptin concentrations: gender differences and associations with metabolic risk factors for cardiovascular disease. *Diabetologia*. 1997;40:1178–1184.
32. **Rider OJ, Francis JM, Ali MK, et al.** Effects of catecholamine stress on diastolic function and myocardial energetics in obesity. *Circulation*. 2012;125:1511–1519.
33. **Lacombe VA, Viatchenko-Karpinski S, Terentyev D, et al.** Mechanisms of impaired calcium handling underlying subclinical diastolic dysfunction in diabetes. *Am J Physiol Regul Integr Comp Physiol*. 2007;293:R1787–R1797.
34. **Weber KT, Brilla CG, Janicki JS.** Myocardial fibrosis: functional significance and regulatory factors. *Cardiovas Res*. 1993;27:341–348.
35. **Burgess ML, Buggy J, Price RL, et al.** Exercise- and hypertension-induced collagen changes are related to left ventricular function in rat hearts. *Am J Physiol*. 1996;270:H151–H159.
36. **DeMarco VG, Johnson MS, Ma L, et al.** Overweight female rats selectively breed for low aerobic capacity exhibit increased myocardial fibrosis and diastolic dysfunction. *Am J Physiol Heart Circ Physiol*. 2012;302:H1667–H1682.
37. **Zhou X, Ma L, Habibi J, et al.** Nebivolol improves diastolic dysfunction and myocardial remodeling through reductions in oxidative stress in the Zucker obese rat. *Hypertension*. 2010;55:880–888.
38. **Rider OJ, Cox P, Tyler D, Clarke K, Neubauer S** 2012 Myocardial substrate metabolism in obesity. *Int J Obes (Lond)*. 2013;37(7): 972–979.
39. **Zhang Y, Yuan M, Bradley KM, Dong F, Anversa P, Ren J.** Insulin-like growth factor 1 alleviates high-fat diet-induced myocardial contractile dysfunction: role of insulin signaling and mitochondrial function. *Hypertension*. 2012;59:680–693.
40. **Mitra R, Nogee DP, Zechner JF, et al.** The transcriptional coactivators, PGC-1α and β, cooperate to maintain cardiac mitochondrial function during the early stages of insulin resistance. *J Mol Cell Cardiol*. 2012;52:701–170.
41. **Holloway GP, Snook LA, Harris RJ, Glatz JF, Luiken JJ, Bonen A.** In obese zucker rats, lipids accumulate in the heart despite normal mitochondrial content, morphology and long-chain fatty acid oxidation. *J Physiol*. 2011;589:169–180.
42. **Padrão AI, Ferreira RM, Vitorino R, et al.** OXPHOS susceptibility to oxidative modifications: the role of heart mitochondrial subcellular location. *Biochim Biophys Acta*. 2011;1807:1106–1113.
43. **Lee J, Xu Y, Lu L, et al.** Multiple abnormalities of myocardial insulin signaling in a porcine model of diet-induced obesity. *Am J Physiol Heart Circ Physiol*. 2010;298:H310–H319.
44. **Ritchie RH, Love JE, Huynh K, et al.** Enhanced phosphoinositide 3-kinase(p110α) activity prevents diabetes-induced cardiomyopathy and superoxide generation in a mouse model of diabetes. *Diabetologia*. 2012;55:3369–3381.
45. **Camper-Kirby D, Welch S, Walker A, et al.** Myocardial Akt activation and gender: increased nuclear activity in females versus males. *Circ Res*. 2001;88:1020–1027.
46. **Zhang YH, Zhang MH, Sears CE, et al.** Reduced phospholamban phosphorylation is associated with impaired relaxation in left ventricular myocytes from neuronal NO synthase-deficient mice. *Circ Res*. 2008;102(2):242–249.
47. **Bender SB, McGraw AP, Jaffe IZ, Sowers JR.** Mineralocorticoid receptor-mediated vascular insulin resistance: an early contributor to diabetes-related vascular disease? *Diabetes*. 2013;62:313–319.
48. **Daniel KR, Wells G, Stewart K, Moore B, Kitzman DW.** Effect of aldosterone antagonism on exercise tolerance, Doppler diastolic function, and quality of life in older women with diastolic heart failure. *Congest Heart Fail*. 2009;15:68–74.
49. **Kosmala W, Przewlocka-Kosmala M, Szczepanik-Osadnik H, Mysiak A, Marwick TH.** Fibrosis and cardiac function in obesity: a randomised controlled trial of aldosterone blockade. *Heart*. 2013; 99:320–326.
50. **Kosmala W, Przewlocka-Kosmala M, Szczepanik-Osadnik H, Mysiak A, O'Moore-Sullivan T, Marwick TH.** A randomized study of the beneficial effects of aldosterone antagonism on LV function, structure, and fibrosis markers in metabolic syndrome. *JACC Cardiovasc Imaging*. 2011;4:1239–1249.
51. **Habibi J, DeMarco VG, Ma L, et al.** Mineralocorticoid receptor blockade improves diastolic function independent of blood pressure reduction in a transgenic model of RAAS overexpression. *Am J Physiol Heart Circ Physiol*. 2011;300:H1484–H1491.